STRUCTURAL BIOLOGY COMMUNICATIONS

ISSN 2053-230X

Expression and crystallographic studies of the *Arabidopsis thaliana* GDP-D-mannose pyrophosphorylase VTC1

Shun Zhao[a,b]* and Lin Liu[a]

[a]Key Laboratory of Photobiology, CAS Center for Excellence in Molecular Plant Sciences, Institute of Botany, Chinese Academy of Sciences, Beijing 100093, People's Republic of China, and [b]University of Chinese Academy of Sciences, Beijing 100049, People's Republic of China. *Correspondence e-mail: zhaoshun2010@ibcas.ac.cn

Received 18 March 2016
Accepted 20 August 2016

Edited by M. L. Pusey, University of Alabama, USA

Keywords: ascorbic acid biosynthesis; GDP-D-mannose pyrophosphorylase; *Arabidopsis thaliana*.

GDP-D-mannose pyrophosphorylase catalyzes the production of GDP-D-mannose, an intermediate product in the plant ascorbic acid (AsA) biosynthetic pathway. This enzyme is a key regulatory target in AsA biosynthesis and is encoded by *VITAMIN C DEFECTIVE 1* (*VTC1*) in the *Arabidopsis thaliana* genome. Here, recombinant VTC1 was expressed, purified and crystallized. Diffraction data were obtained from VTC1 crystals grown in the absence and presence of substrate using X-rays. The ligand-free VTC1 crystal diffracted X-rays to 3.3 Å resolution and belonged to space group $R32$, with unit-cell parameters $a = b = 183.6$, $c = 368.5$ Å, $\alpha = \beta = 90$, $\gamma = 120^\circ$; the crystal of VTC1 in the presence of substrate diffracted X-rays to 1.75 Å resolution and belonged to space group $P2_1$, with unit-cell parameters $a = 70.8$, $b = 83.9$, $c = 74.5$ Å, $\alpha = \gamma = 90.0$, $\beta = 114.9^\circ$.

1. Introduction

Ascorbic acid (AsA), or vitamin C, commonly functions as an antioxidant and enzymatic cofactor in animals and plants (Englard & Seifter, 1986; Smirnoff, 2000; Foyer & Noctor, 2011). Plants are the major AsA source for humans, in which the gene encoding the last enzyme in the AsA-biosynthetic pathway is mutated and its product is nonfunctional (Chatterjee, 1973). AsA also plays a key role in plant growth and development by enhancing plant tolerance to various stresses (Hemavathi *et al.*, 2010; Tóth *et al.*, 2011; Vacca *et al.*, 2004).

The major AsA-biosynthetic pathway in plants starts from GDP-D-mannose (Smirnoff *et al.*, 2001). This differs from AsA biosynthesis in most animals and the alternative pathway in plants and *Euglena*, which starts from UDP-D-glucose (Linster & van Schaftingen, 2007; Wheeler *et al.*, 2015). VITAMIN C DEFECTIVE 1 (VTC1)/CYTOKINESIS DEFECTIVE 1 (CYT1), hereafter referred to as VTC1, is a GDP-D-mannose pyrophosphorylase (GMPP) in the model plant *Arabidopsis thaliana* (Conklin *et al.*, 1997; Nickle & Meinke, 1998; Lukowitz *et al.*, 2001). VTC1 catalyzes the conversion of D-mannose 1-phosphate to GDP-D-mannose, the first rate-limiting step of the major AsA-biosynthetic pathway in plants (Wheeler *et al.*, 1998). In the *vtc1* mutant, the AsA level decreases 70% compared with the wild type (Conklin *et al.*, 1997, 1999). VTC1 is tightly regulated by multiple mechanisms. At the transcriptional level, ETHYLENE RESPONSE FACTOR 98 acts as a positive regulator of VTC1 (Zhang *et al.*, 2012). At the post-translational level, the photomorphogenic factor

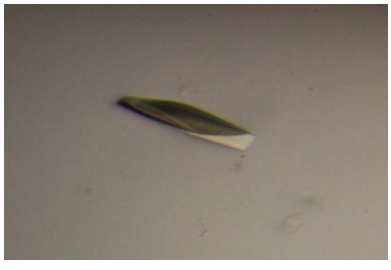

COP9 signalosome subunit 5B interacts with VTC1 and promotes VTC1 degradation though proteasomes in the dark (Wang, Yu *et al.*, 2013; Wang, Zhang *et al.*, 2013). Recently, two VTC1 stimulators, KONJAC1 and KONJAC2, have been identified (Sawake *et al.*, 2015). Both proteins can interact with VTC1 and enhance its GMPP activity.

Despite the accumulated physiological studies of VTC1, the structural basis of the catalytic activity of this enzyme and its regulation is still unknown. Here, we report the purification, crystallization and diffraction of ligand-free VTC1 and VTC1 in the presence of its substrate.

2. Materials and methods

2.1. Protein expression and purification

The full-length gene for VTC1 (AT2G39770) was amplified from an *A. thaliana* cDNA library by PCR and was ligated into the pEASY-Blunt simple cloning vector (TransGen Biotech, People's Republic of China). The gene was inserted into the expression vector pET-28a(+) (Novagen) between NcoI and HindIII sites. The resulting plasmid encodes C-terminally His_6-tagged VTC1. This plasmid was transformed into *Escherichia coli* strain BL21(DE3) and the cells were cultured in LB medium. When the cell density reached an OD_{600} of 0.6–0.8, protein expression was introduced with 0.2 m*M* isopropyl *β*-D-1-thiogalactopyranoside and the cells were grown at 289 K for 16 h. The cells were then harvested by centrifugation (5000*g*, 10 min) and resuspended in buffer *A* (20 m*M* Tris–HCl pH 7.5, 150 m*M* NaCl) supplemented with 20 m*M* imidazole. The cells were disrupted by ultrasonication on ice and were centrifuged at 30 000*g* for 30 min. The supernatant was loaded onto a pre-equilibrated Ni^{2+}–nitrilotriacetic acid column (Qiagen) and the unbound protein was washed with buffer *A* supplemented with 20 m*M* imidazole. The recombinant protein was subsequently eluted with buffer *A* supplemented with 200 m*M* imidazole. The protein was further purified by gel-filtration chromatography using a HiLoad 16/60 Superdex 200 column (GE Healthcare) pre-equilibrated with buffer *A*. The elution peak was collected, pooled and concentrated by ultrafiltration with a 30 kDa cutoff centrifugal filter (Millipore). The purity and concentration were determined by

Table 1
VTC1 construction and expression information.

Source organism	*A. thaliana*
DNA source	cDNA
Forward primer	CATGCCATGGGCATGAAGGCACTCATTCTTGTTG
Reverse primer	CCCAAGCTTCATCACTATCTCTGGCTTCAAGAT
Cloning vector	pEASY-Blunt simple cloning vector
Expression vector	pET-28a(+)
Expression host	*E. coli* BL21(DE3)
Complete amino-acid sequence of the construct produced	MGMKALILVGGFGTRLRPLTLSFPKPLVDFANKP- MILHQIEALKAVGVDEVVLAINYQPEVMLNFL- KDFETKLEIKITCSQETEPLGTAGPLALARDK- LLDGSGEPFFVLNSDVISEYPLKEMLEFHKSH- GGEASIMVTKVDEPSKYGVVVMEESTGRVEKF- VEKPKLYVGNKINAGIYLLNPSVLDKIELRPT- SIEKETFPKIAAAQGLYAMVLPGFWMDIGQPR- DYITGLRLYLDSLRKKSPAKLTSGPHIVGNVL- VDETATIGEGCLIGPDVAIGPGCIVESGVRLS- RCTVMRGVRIKKHACISSSIIGWHSTVGQWAR- IENMTILGEDVHVSDEIYSNGGVVLPHKEIKS- NILKPEIVMKLAAALEHHHHHH

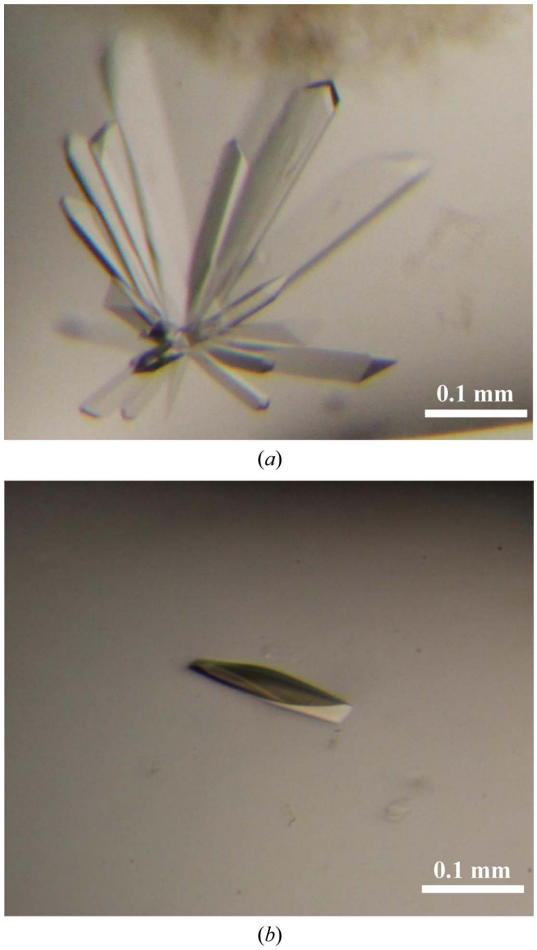

Figure 1
Crystals of ligand-free VTC1 and co-crystallized VTC1. (*a*) Crystal of ligand-free VTC1 obtained using 0.1 *M* bis-tris pH 6.5, 25%(*w*/*v*) PEG 3350, 0.2 *M* lithium sulfate; (*b*) crystal of VTC1 in the presence of GTP and D-mannose 1-phosphate obtained using 0.1 *M* magnesium formate, 15%(*w*/*v*) PEG 3350.

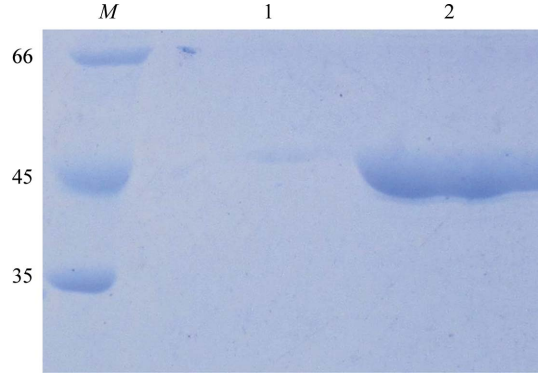

Figure 2
SDS–PAGE analysis of a crystal of VTC1 grown in the presence of substrate. Lane *M*, molecular-weight markers (labelled in kDa); lane 1, buffer used to wash the crystals; lane 2, crystal sample of VTC1 grown in the presence of substrate.

Table 2
Crystallization of ligand-free VTC1 and co-crystallized VTC1.

	Ligand-free VTC1	Co-crystallized VTC1
Method	Sitting-drop vapour diffusion	Sitting-drop vapour diffusion
Plate type	48-well plates, Hampton Research	48-well plates, Hampton Research
Temperature (K)	289	289
Protein concentration (mg ml^{-1})	7.5	7.5
Buffer composition of protein solution	20 m*M* Tris–HCl pH 7.5, 150 m*M* NaCl	20 m*M* Tris–HCl pH 7.5, 150 m*M* NaCl
Composition of reservoir solution	0.1 *M* bis-tris pH 6.5, 25%(*w*/*v*) PEG 3350, 0.2 *M* lithium sulfate	0.1 *M* magnesium formate, 15%(*w*/*v*) PEG 3350
Volume and ratio of drop	2 µl, 1:1	2 µl, 1:1
Volume of reservoir (µl)	200	200

SDS–PAGE and a Bradford assay, respectively. The expression information is given in Table 1.

2.2. Crystallization

The sitting-drop vapour-diffusion technique was used for crystallization screening. The initial crystallization conditions for VTC1 without ligands were screened at 277 and 289 K using concentrations of 7.5 and 15 mg ml^{-1}, respectively. The process was carried out by mixing protein and reservoir solution in a 1:1 volume ratio. The ligand-free VTC1 crystal was grown using 0.1 *M* bis(2-hydroxyethyl)iminotris(hydroxymethyl)methane (bis-tris) pH 6.5, 25%(*w*/*v*) PEG 3350, 0.2 *M* lithium sulfate. The co-crystallization of VTC1 with GTP and D-mannose 1-phosphate was set up as for ligand-free VTC1. The VTC1 protein was incubated with GTP and D-mannose 1-phosphate in a 1:5:5 molar ratio on ice for 1 h. The co-crystallized VTC1 crystal was grown in 0.1 *M* magnesium formate, 15%(*w*/*v*) PEG 3350.

2.3. Data collection

All of the crystals were transferred to crystallization buffer supplemented with 10% glycerol for 30 s and flash-cooled in liquid nitrogen. All diffraction data were collected on beamline BL17U at Shanghai Synchrotron Radiation Facility at a wavelength of 0.9793 Å at 100 K and were recorded on an ADSC Quantum 315r detector with 0.5 s exposure for every 1° oscillation (Wang *et al.*, 2015). All data sets were processed, integrated and scaled with *DENZO* and *SCALEPACK* in the *HKL*-2000 package (Otwinowski & Minor, 1997).

3. Results and discussion

To investigate the mechanism of catalysis by VTC1, we produced and crystallized full-length ligand-free VTC1 (Fig. 1*a*). We also obtained crystals of VTC1 in the presence of GTP and D-mannose 1-phosphate (Fig. 1*b*). Because VTC1 crystals in the presence of substrate were obtained in a condition containing Mg^{2+}, an activator of VTC1, the protein

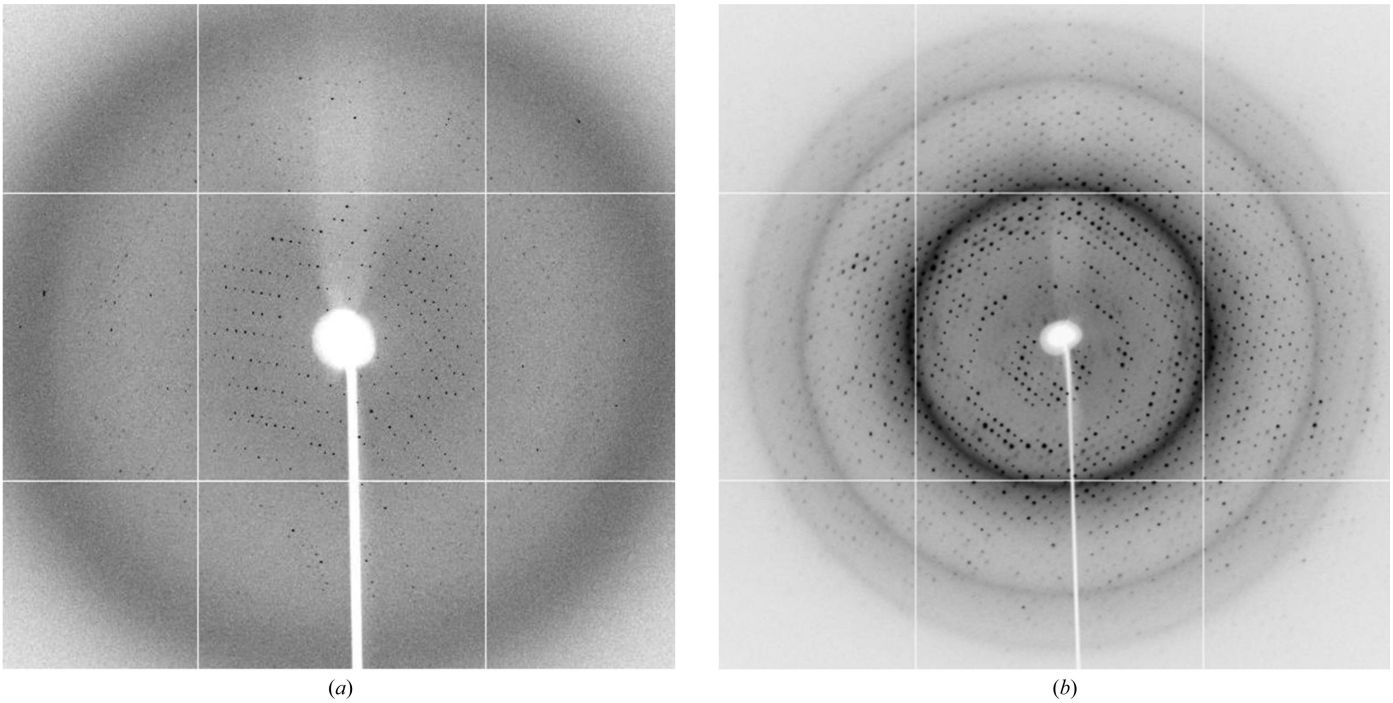

(*a*) (*b*)

Figure 3
The X-ray diffraction patterns of a ligand-free VTC1 crystal and a VTC1 crystal grown in the presence of substrate. (*a*) Diffraction image of ligand-free VTC1 to a resolution of 3.3 Å; (*b*) diffraction image of VTC1 in the presence of GTP and D-mannose 1-phosphate to a resolution of 1.75 Å.

Table 3
Data collection and processing.

	Ligand-free VTC1	Co-crystallized VTC1
Diffraction source	BL17U, SSRF	BL17U, SSRF
Wavelength (Å)	0.9793	0.9793
Temperature (K)	100	100
Detector	ADSC Q315r	ADSC Q315r
Crystal-to-detector distance (mm)	400	120
Rotation range per image (°)	1	1
Total rotation range (°)	100	180
Exposure time per image (s)	0.5	0.5
Space group	$R32$	$P2_1$
a, b, c (Å)	183.6, 183.6, 368.5	70.8, 83.9, 74.5
α, β, γ (°)	90.0, 90.0, 120.0	90.0, 114.9, 90.0
Mosaicity (°)	0.54	0.32
Resolution range (Å)	50–3.30 (3.42–3.30)	50.0–1.75 (1.81–1.75)
Total No. of reflections	201448	300113
No. of unique reflections	36128	78685
Completeness (%)	99.5 (99.6)	98.6 (97.6)
Multiplicity	5.6 (5.7)	3.8 (3.8)
$\langle I/\sigma(I)\rangle$	14.0 (3.1)	21.5 (2.5)
$R_{\rm r.i.m.}$†	0.126 (0.598)	0.069 (0.648)
$R_{\rm merge}$‡	0.115 (0.544)	0.087 (0.906)

† $R_{\rm r.i.m.} = \sum_{hkl}\{N(hkl)/[N(hkl)-1]\}^{1/2}\sum_i |I_i(hkl) - \langle I(hkl)\rangle|/\sum_{hkl}\sum_i I_i(hkl)$, where $I_i(hkl)$ is the intensity of the ith measurement of an equivalent reflection with indices hkl. ‡ $R_{\rm merge} = \sum_{hkl}\sum_i |I_i(hkl) - \langle I(hkl)\rangle|/\sum_{hkl}\sum_i I_i(hkl)$, where $I_i(hkl)$ is the ith observation of reflection hkl and $\langle I(hkl)\rangle$ is the weighted intensity for all observations i of reflection hkl.

molecules in solution may contain product molecules. The crystallization information is listed in Table 2.

We also confirmed the integrity of the VTC1 protein in the co-crystallized crystals. Crystals were picked up from the drop, washed with reservoir solution, dissolved in SDS–PAGE loading buffer and subsequently checked by SDS–PAGE. It showed only a single band near to 45 kDa (Fig. 2), which corresponds to the molecular weight of VTC1. This band was then identified by the peptide mass fingerprinting method, with a top score of 198 and a sequence coverage of 61%.

Two data sets were collected and the statistics of data collection are summarized in Table 3. The ligand-free VTC1 crystal diffracted X-rays to 3.3 Å resolution (Fig. 3*a*) and its space group is $R32$, which differs from that of the crystal of co-crystallized VTC1, with unit-cell parameters $a = b = 183.6$, $c = 368.5$ Å, $\alpha = \beta = 90$, $\gamma = 120°$. The VTC1 crystals grown in the presence of substrate diffracted to a high resolution of 1.75 Å (Fig. 3*b*), with space group $P2_1$ and unit-cell parameters $a = 70.8$, $b = 83.9$, $c = 74.5$ Å, $\alpha = \gamma = 90.0$, $\beta = 114.9°$. We are working towards phase solution by single-wavelength anomalous dispersion using selenomethionine-containing crystals.

Acknowledgements

We thank the staff at Shanghai Synchrotron Radiation Facility for technical support during data collection. This work was supported by the National Natural Science Foundation of China (Grant No. 31170688).

References

Chatterjee, I. B. (1973). *Science*, **182**, 1271–1272.
Conklin, P. L., Norris, S. R., Wheeler, G. L., Williams, E. H., Smirnoff, N. & Last, R. L. (1999). *Proc. Natl Acad. Sci. USA*, **96**, 4198–4203.
Conklin, P. L., Pallanca, J. E., Last, R. L. & Smirnoff, N. (1997). *Plant Physiol.* **115**, 1277–1285.
Englard, S. & Seifter, S. (1986). *Annu. Rev. Nutr.* **6**, 365–406.
Foyer, C. H. & Noctor, G. (2011). *Plant Physiol.* **155**, 2–18.
Hemavathi, Upadhyaya, C. P., Akula, N., Young, K. E., Chun, S. C., Kim, D. H. & Park, S. W. (2010). *Biotechnol. Lett.* **32**, 321–330.
Linster, C. L. & Van Schaftingen, E. (2007). *FEBS J.* **274**, 1–22.
Lukowitz, W., Nickle, T. C., Meinke, D. W., Last, R. L., Conklin, P. L. & Somerville, C. R. (2001). *Proc. Natl Acad. Sci. USA*, **98**, 2262–2267.
Nickle, T. C. & Meinke, D. W. (1998). *Plant J.* **15**, 321–332.
Otwinowski, Z. & Minor, W. (1997). *Methods Enzymol.* **276**, 307–326.
Sawake, S., Tajima, N., Mortimer, J. C., Lao, J., Ishikawa, T., Yu, X., Yamanashi, Y., Yoshimi, Y., Kawai-Yamada, M., Dupree, P., Tsumuraya, Y. & Kotake, T. (2015). *Plant Cell*, **27**, 3397–3409.
Smirnoff, N. (2000). *Curr. Opin. Plant Biol.* **3**, 229–235.
Smirnoff, N., Conklin, P. L. & Loewus, F. A. (2001). *Annu. Rev. Plant Physiol. Plant Mol. Biol.* **52**, 437–467.
Tóth, S. Z., Nagy, V., Puthur, J. T., Kovács, L. & Garab, G. (2011). *Plant Physiol.* **156**, 382–392.
Vacca, R. A., de Pinto, M. C., Valenti, D., Passarella, S., Marra, E. & De Gara, L. (2004). *Plant Physiol.* **134**, 1100–1112.
Wang, J., Yu, Y., Zhang, Z., Quan, R., Zhang, H., Ma, L., Deng, X. W. & Huang, R. (2013). *Plant Cell*, **25**, 625–636.
Wang, J., Zhang, Z. & Huang, R. (2013). *Plant Signal. Behav.* **8**, e24536.
Wang, Q.-S. *et al.* (2015). *Nucl. Sci. Tech.* **26**, 010102.
Wheeler, G., Ishikawa, T., Pornsaksit, V. & Smirnoff, N. (2015). *Elife*, **4**, e06369.
Wheeler, G. L., Jones, M. A. & Smirnoff, N. (1998). *Nature (London)*, **393**, 365–369.
Zhang, Z., Wang, J., Zhang, R. & Huang, R. (2012). *Plant J.* **71**, 273–287.